Small Scale Volumetric Inhomogeneities of Shallow Water Sediments: Measurements and Discussion

Dajun Tang

Applied Physics Laboratory
University of Washington
1013 NE 40th Street
Seattle, WA 98105, USA
E-mail: djtang@apl.washington.edu

Abstract

There is a consensus that high-frequency acoustic scattering by the ocean bottom is partly due to sediment volumetric inhomogeneities, i.e., random fluctuations in sediment sound speed and density. Understanding the spatial distribution and temporal variability of such inhomogeneities at the centimeter scale is of great importance to modeling and predicting sound interaction with shallow water sediments. Core data provide only sediment variability in depth, which is not sufficient for determining sound scattering, since fluctuations of sediment parameters versus horizontal dimensions are also needed. Efforts were made to measure sound speed and porosity variabilities of sediments using techniques based on acoustic tomography and microelectric conductivity. While the results are still preliminary, it is clear from the available data that sediment inhomogeneity is a general phenomenon, and measurements such as those reported here will make it possible to conduct unambiguous model-data comparisons in future high-frequency bottom-scattering experiments.

1. Introduction

Natural sedimentation processes make sediment parameters, such as the compressional and shear speeds, density, and attenuation coefficients, deviate from stratification in a random fashion, and such deviations will cause sound to scatter. Conventionally, these deviations are divided into two categories: water-bottom interface roughness and sediment volume inhomogeneities, which include all variabilities other than the roughness. While the roughness issue has been extensively studied both theoretically and experimentally, it is only relatively recently that scattering by volume inhomogeneities has started to receive serious attention. This paper is devoted to the issues concerning the measurement of volume inhomogeneities in sediments. While rocks, shell pieces, and gas bubbles in sediments can be significant contributors to scattering, they should be studied as separate subjects. We confine the discussion in this paper to scattering due to the fluctuating medium parameters of the bottom.

Since it is impractical to measure the details of the sediment volume inhomogeneities deterministically, to study sediment volume scattering, a statistical approach is often used to study the average intensity of the scattered sound. References on modeling sediment volume scattering can be found in [1]–[7]. These models are based on a first-order perturbation approximation of the wave equation, and the sediment is assumed to be a fluid medium. Recently, Ivakin and Jackson [8] showed that for a sedimented bottom, a fluid model is an excellent approximation in treating scattering problems. When the sediment is modeled as a fluid medium, there are three acoustic parameters that determine the scattering process. They are the sediment sound speed, density, and attenuation coefficient. While it is not certain that the attenuation coefficient is a constant over space for a given frequency, it is potentially a scatterer. However, since attenuation manifests itself in the wave equation as the imaginary part of the wavenumber for a given frequency, and it is known that the imaginary part of the wavenumber is much smaller than the real part for almost all sediments concerned, scattering due to the random fluctuation of the attenuation coefficient is a second-order effect at best compared with that due to the fluctuations of sound speed and density. Thus, the sound speed and density are the only parameters left to be determined. If we assume that the sound speed and density fluctuate randomly in three-dimensional space around their mean profiles, the

first-order scattering cross section is completely determined if the auto- and cross-correlation functions of the two random quantities are known [1, 4]. In order to compare measured high-frequency scattering strengths to model predications, it is essential to have measurements of these correlation functions that are accurate to sub-wavelength scales. These correlation functions could be estimated from core data. But cores provide only depth information; estimation of correlation functions from such cores can result in error because (1) variabilities in depth can be due to fine, flat layering, which does not cause scattering, and (2) the statistical characteristics of variability in the horizontal direction can be quite different from those in depth. In the following, two efforts aimed at providing horizontal, as well as depth, data for estimating the correlation functions of sound speed and density in sediments are presented. The section on sediment microconductivity presents a method to measure porosity fluctuations, and therefrom, density fluctuations. The section on acoustic tomography presents a method for measuring sediment sound speed variability.

2. Sediment Microconductivity

Seawater is a conducting medium whereas the sediment solids themselves usually are made of poorly conducting materials. Thus, sediment electric conductivity, or equivalently its reciprocal, resistivity, is a measure of sediment porosity. When sediment porosity is known, sediment density can be obtained from the densities of the seawater and the sediment grains, quantities that are relatively easy to measure. Archie [9] proposed the following empirical relationship between conductivity and porosity:

$$F = \frac{c_w}{c_s} = \phi^{-n}, \tag{1}$$

where ϕ is porosity, F is a "formation" factor which is the ratio of the conductivity of the interstitial water, c_w, to that of the sediment, c_s, and the parameter n is a constant depending on the type of the sediment being measured. Later, in order to better fit data, Archie's formula was modified to include an additional parameter, a, which depends on the distribution of sediment particle sizes [10]:

$$F = \frac{c_w}{c_s} = a \cdot \phi^{-n}. \tag{2}$$

It can be understood that the conductivity of sediments depends on the shape and packing structure of the sediment grains because they will decide the passageways for charges to go through. For sediments made of identical spherical particles, there is a theoretical predication of the relation between porosity and conductivity [11]. However, theoretical relations are not available for real sediments owing to the complexity of the grain size composition and packing. In practice, the constants n and a are determined using an independent method for each sediment.

Conventional conductivity probes consist of a single sensor which can measure conductivity versus depth [12]. In order to measure density variability in the horizontal as well as in depth, we are developing a multi-sensor conductivity probe. Figure 1 is a schematic of the probe system. It consists of 16 equally spaced (1 cm), identical probe tips made of platinum spheres with a diameter of 0.6 mm, which ensures that the spatial resolution of each tip will be better than 1 m^3. By mechanically controlling the penetration depth of the probe into the sediments, we will be able to obtain a two-dimensional data set of sediment conductivity, and from that an estimation of the two-dimensional variability of the sediment porosity using (2). The system has been tested and calibrated in the laboratory using shallow-water sediment samples obtained from cores. First, the conductivity of sediment samples and that of the overlaying water were measured using the probe, and the porosity of the samples was estimated using (2). The porosity of the samples was also measured independently by weighing the samples while wet and after drying. Owing to space limitations, we will not give the details of the calibration process in this paper.

We have used this probe to measure the conductivity of a few sediment cores obtained off the Northern California coast in the summer of 1996. Figure 2a is one example of the measured data. The figure shows the reciprocal of the formation factor, or the ratio of sediment conductivity to that of overlaying water, plotted against depth for the 16 channels. The result is unity during the first few millimeters, indicating the probe was measuring the seawater just above the sediment. The sediment conductivity decreases quickly over depth in the next few millimeters and then stabilizes. Since there are 16 channels on the probe, the horizontal variability is obtained over a width of 15 cm. Figure 2b shows the mean profile of the conductivity averaged over the 16 channels and the mean porosity profile estimated from the mean conductivity profile. The parameters used to convert conductivity to porosity were taken from [13] based on empirical data. One of the advantages of having two-dimensional data is that we can estimate the depth-dependent mean profiles as shown here. Let the two dimensional porosity data be $p(x, z)$ and the mean porosity profile be $P(z) = \langle p(x, z) \rangle$; we define the normalized fluctuation ϵ_p as

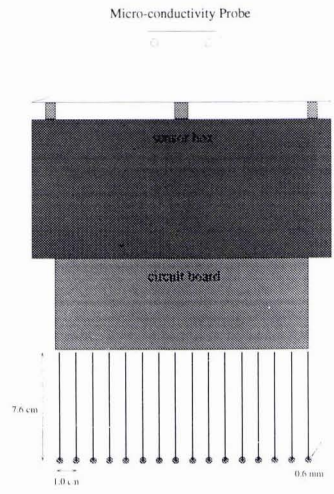

Figure 1: Configuration of the Conductivity Probe

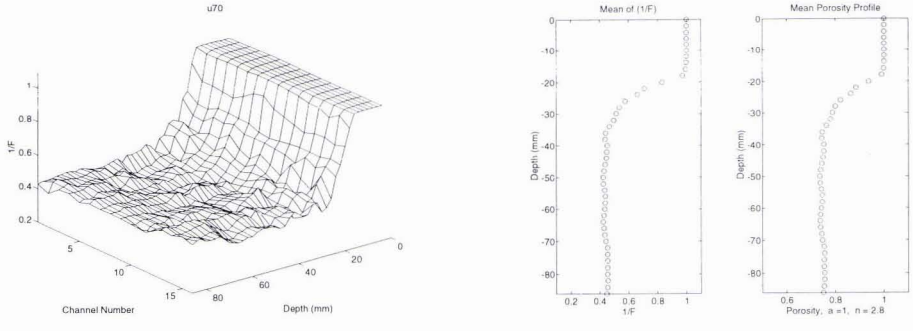

(a) Two-dimensional data

(b) Mean profiles

Figure 2: Example of 2-D conductivity data and mean profiles averaged across all 16 channels; core u70.

$$\epsilon_p = \frac{p(x,z) - P(z)}{P(z)}. \tag{3}$$

As stated in the Introduction, this is one of the two quantities for which we want to estimate the spectra.

One of the interesting questions is whether ϵ_p is spatially stationary. Since the mean profile is depth dependent, the stationarity of ϵ_p over depth is of special concern. Figure 3 shows three different sets of porosity variability data. There is no apparent depth or horizontal dependence in any of the three. Therefore we conclude that in these particular sets of data the porosity variability is spatially stationary. When a random process is stationary, its correlation function depends only on the difference coordinates, and its power spectrum is the quantity that is the input to first-order scattering models [1]. Next, we estimate the two-dimensional power spectrum of ϵ_p. The power spectrum is obtained by averaging the square of the absolute value of the Fourier transform from all data sets. Figure 4 is the estimated power spectrum. In this particular case, the two-dimensional power spectrum is isotropic. Hence, assuming that the three-dimensional power spectrum is isotropic in the horizontal dimensions as well, we can estimate it through its one-dimensional power spectrum [14]. Figure 5 shows an averaged one-dimensional power spectrum and a fit to a power-law spectrum of the form:

$$W_1(k) = \frac{w_1}{k^{m_1}}, \tag{4}$$

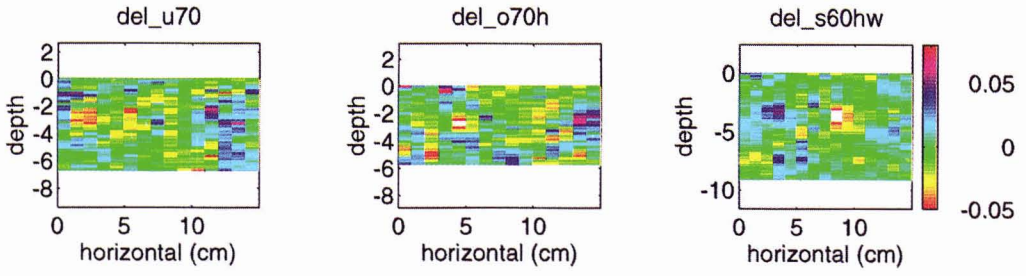

Figure 3: Porosity variability, ϵ_p, data of three cores, u70, o70h, and s60hw.

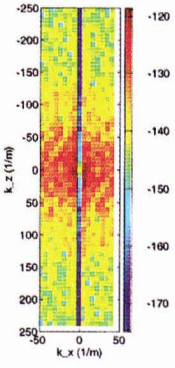

Figure 4: Two-dimensional power spectrum obtained from averaging multiple core data.

where $w_1 = 1.1 \times 10^{-6}$ and $m_1 = 1.7$. Based on this result, the isotropic three-dimensional power spectrum is

$$W(k) = \frac{w_3}{k^{m_3}}, \tag{5}$$

with $w_3 = 2.9 \times 10^{-7}$ and $m_3 = 3.7$. Here we have demonstrated the capabilities of the sediment microconductivity probe in providing data for estimating the sediment porosity power spectrum. While encouraging, we emphasize that these results are preliminary and a field version of the probe is yet to be built that will be able to provide *in situ* data.

3. Acoustic Tomography

Now we shift our attention to sound speed measurement. In order to measure *in situ* sediment sound speed variability in both horizontal and depth dimensions, acoustic tomography is a natural choice. Yamamoto [14] has conducted a series of tomographic measurements. Here we present an acoustic tomographic system specifically designed to measure *in situ* sediment sound-speed variabilities to support modeling of high-frequency bottom-scattering work.

The *in situ* sediment acoustic imaging system consists of an array of needle-like probes that can be pressed into the sediment, where each probe is a vertical line array of acoustic transducers. The current system consists of three identical probes attached to a sturdy frame and connected to a subsea electronics pressure housing. Two probes are oriented vertically and pressed into the sediment about 1 m apart; the third is oriented horizontally, just above the seafloor, between the two vertical probes (see Figure 6). Since these probes are all aligned on a common plane, the current system is capable of only two-dimensional imaging. Eventually, more probes may be added to obtain three dimensional data. Each probe contains 20 acoustic transducers, arranged as a line array with 5-cm spacing. Thus the active area is approximately 1 m long on each side. Each transducer in every probe is capable of both transmit and receive. An internal multiplexer in the probe is used to select a single transducer so that the number of wires in the cabling is minimized. The probes are connected to the subsea electronics module which

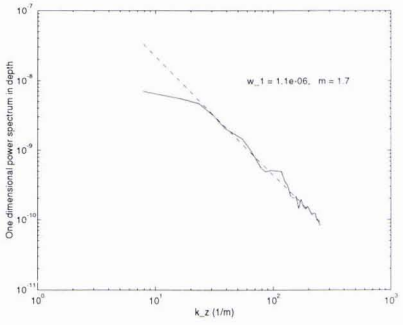

Figure 5: One-dimensional power spectrum in depth and a fit to a power-law spectrum.

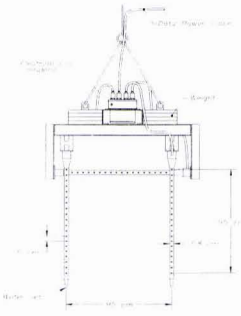

Figure 6: Configuration of the sediment tomography probe system.

contains a transmitter, a receiver, and a microcontroller for multiplexer and gain control. A multi-conductor cable extends to the surface. This cable connects to a PC via an analog input for data acquisition and to a serial port for multiplexer control. A small power supply is the only other surface equipment required to operate the subsea electronics. Individual transducers are selected by the PC software for transmit and receive, and a ping is initiated. This design allows 1200 direct raypaths between pairs of transducers and receivers. Figure 7 demonstrates some of the ray paths crisscross the 1 m^2 area.

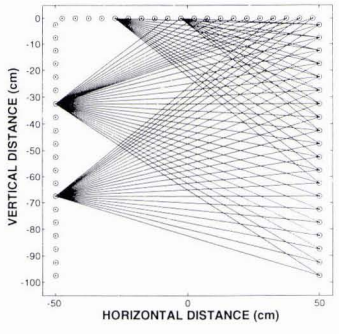

Figure 7: Sample ray paths of the sediment tomographic system.

All possible raypath combinations between the probes are sequentially interrogated. The objective is to accurately estimate the travel time from transmit to receive on each ray path. Data are acquired by an analog-to-digital data acquisition board plugged into the PC. A Windows based application program has been written to control the multiplexer for transducer selection and to acquire and store the raw sonar data. The resulting set of average sound velocities forms the input to the tomography processing algorithm.

The transducers used are free-flooded cylinders, with a resonant frequency of 100 kHz and a bandwidth of approximately 40 kHz. These cylinders have a torroidal beam pattern, and therefore are oriented with their longitudinal axes perpendicular to that of the probe itself, so that their beam patterns are aligned with the imaging plane. The elements are potted in polyurethane and suspended between two high-strength steel stiffening bars. The diameter of the probe is 1.5 in., expanded slightly at the top to accommodate the interface circuitry and connector pigtail. A long, thin printed circuit board extends along the entire length of the probe, outside of one of the steel bars. Also encapsulated in the polyurethane is a stainless steel tube connected to the probe tip to allow use of a water jet for assistance in penetrating difficult sediment.

One experiment was conducted at the Hadley Harbor near Woods Hole, Massachusetts, on November 15, 1996, on the vessel *Asterias* belonging to the Woods Hole Oceanographic Institution. First, a set of calibration data were obtained when the entire system was in the water column. Then two divers guided the system into sediments. There were two deployments about a mile apart, both in soft clay sediments. The probe system worked flawlessly and easily penetrated into the sediment at these muddy sites without use of the water jet. Although we could not tell the difference between the two sites by visually examining the sediment samples, the first location allowed little sound transmission, whereas the second provided clear data with better quality than expected. It is hypothesized that large amount of gas might have been present at the first location so sound waves were prevented from going through the 1 m course. However, further measurement is needed to verify this hypothesis.

Figure 8 shows some selected channels of time-series data. In this figure, the transmitter is the tenth element from the bottom on the left vertical probe, and the receivers are all the 20 hydrophones on the other vertical probe. On the left is a set of calibration data recorded when the system was suspended in the water column. On the right are actual time series on the hydrophones corresponding to those as on the left. The signal gain was 8 and the signal level in the figure was normalized, with the highest channel having a value of 100. Signal levels in other channels relative to the highest one are given in the figure on the right. The normalization factor is 2.13. The arrival-time changes relative to the calibration data were picked up and used in a back-projection algorithm to invert for the sound speed in the sediment. Figure 9 is the inverted sound-speed image.

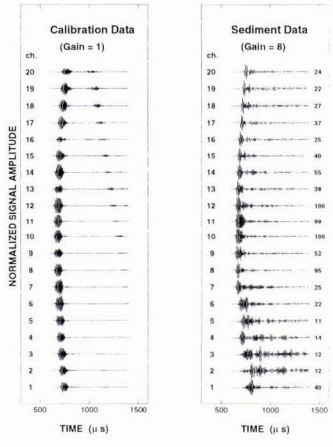

Figure 8: Field experiment time series. (left) calibration data; (right) data measured in the sediment.

The pixel size of the image is 5 cm by 5 cm. The mean sound speed is 1480 m/s. The variability is moderate in the upper half meter, whereas the lower half shows large variabilities. An examination of time series such as those shown in Figure 8 reveals that, in addition to the direct arrivals, there are multiple later arrivals with considerable amplitude. Clearly they are the result of forward scattering due to the presence of yet unknown scatterers. Further, note that the amplitudes of the direct arrivals on the lower hydrophones are considerably smaller than those on the upper ones, indicating a strong attenuating mechanism at work. It is known that when gas is present, the

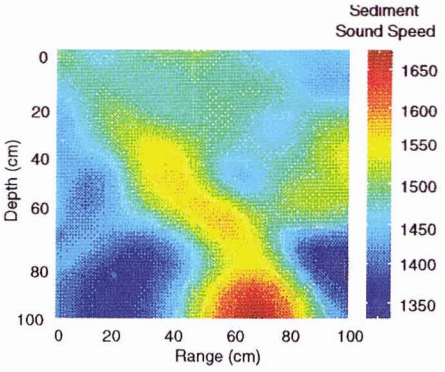

Figure 9: Inverted two-dimensional sound speed variation from field data.

effective sound speed will be markedly reduced. Indeed, in the lower half of the image, the inverted sediment sound speed is much lower than that in the water column. Therefore, we hypothesize that there was gas present in the sediment. From the arrival amplitudes, we estimated the attenuation coefficient as a function of depth. The result is given in Figure 10. Since in the estimation we used the amplitudes of the first arriving peak, and the transmitted signal is an up-chirp starting at 80 kHz, the attenuation coefficient is that at 80 kHz only. While the attenuation coefficient is about 25 dB/m in the upper half, a common value for this type of clay sediment, it jumps to 65 dB/m in the lower half. At two of the hydrophones, the first arrivals were so small that we could not reliably estimate the amplitude at all. Such a high attenuation coefficient is rare except when gas is present. To verify the presence of gas, a new experiment will be conducted at the same site in the next phase along with coring and gas-catching measurements.

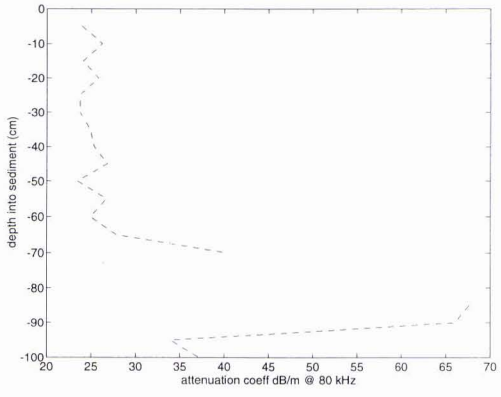

Figure 10: Estimated attenuation coefficient versus depth from field data.

4. Discussion

Two major issues need to be worked on concerning the conductivity probe. The first is the frailty of the tips of the probe. While the resolution requirement forces the tips to be small, it is mechanically difficult to make its structure sturdy enough to withstand repeated field deployment. The second issue is on converting conductivity to porosity. Although empirical relations such as (2) have been used extensively, a systematic verification of their applicability is yet to be done. Finding the relation between the conductivity and the tortuosity of the sediments in addition to porosity would also be potentially fruitful.

While the tomographic instrument works as designed, an increase in its spatial resolution would be desirable. Currently, its resolution is about 5 cm, too coarse compared with that of the conductivity probe, which is 1 cm.

As a result, we cannot resolve the issue of the cross correlation between sound speed and density. In addition, deployment of this system in sandy sediments remains to be tested.

In summary, we have developed two systems for the purpose of supporting modeling of high-frequency bottom scattering by sediment volume inhomogeneities. With such instruments, two-dimensional data on sediment variabilities can be obtained, and a model-data comparison with no free parameters is possible. Conducting a comprehensive high-frequency bottom-scattering experiment along with measurements of the environmental parameters using such instruments as described here, a clear understanding of the bottom scattering process can be expected.

Acknowledgments

The following people made major contributions to the conductivity probe: Neil L. Brown, Jia-Qin Zhang of the Woods Hole Oceanographic Institution, and Daniel G. Frisk of MIT who was working under a summer research program at WHOI. Dr. Robert A. Wheatcroft provided the core data for measuring conductivity.

Dr. Dezhang Chu, Thomas A. Austin, and Alan A. Hinton of WHOI are the principle co-workers on the tomographic system.

This work has been supported by the Office of Naval Research.

References

[1] Jackson, D. R., K. B. Briggs, K. L. Williams, and M. D. Richardson, "Tests of models for high-frequency seafloor backscatter," *IEEE J. Oceanic Engineering*, vol. 21, No. 4, pp. 458-470, October 1996.

[2] A. P. Lyons, A. L. Anderson, and F. S. Dwan, "Acoustic scattering from the seafloor: Modeling and data comparison," *J. Acoust. Soc. Am.*, vol. 95, pp. 2441-2451, May 1994.

[3] Jackson, D. R. and K. B. Briggs, "High-frequency bottom backscattering: Roughness versus sediment volume scattering," *J. Acoust. Soc. Am.*, vol. 92, pp. 962-977, August 1992.

[4] P. D. Mourad and D. R. Jackson, "High frequency sonar equation models for bottom backscatter and forward loss," *Proc. OCEANS '89*, IEEE vol. 4, pp. 1168-1175, September 1989.

[5] D. R. Jackson, D. P. Winebrenner, A. Ishimaru, "Application of the composite roughness model to high-frequency bottom scattering," *J. Acoust. Soc. Am.*, vol. 79, pp. 1410-1422, May 1986.

[6] An. N. Ivakin and Yu. P. Lysanov, "Theory of underwater sound scattering by random inhomogeneities of the bottom," *Sov, Phy. Acoust.*, vol. 27, pp. 61-64, 1981.

[7] P. C. Hines, "Theoretical model of acoustic backscattering from a smooth seabed," *J. Acoust. Soc. Am.*, vol. 88, pp. 325-334, July 1990.

[8] A. N. Ivakin and D. R. Jackson, unpublished (submitted to *J. Acoust. Soc. Am.*).

[9] G. E. Archie, "The electrical resistivity log as an aid in determining some reservoir characteristics," *Trans. AIME*, vol. 146, pp. 54-62, 1942.

[10] V. N. Dakhnov, "Geophysical well logging," *Quarterly of the Colorado School of Mines*, pp. 57, 1962.

[11] P. N. Sen, C. Scala, and M. H. Cohen, "A self-similar model for sedimentary rocks with application to the dielectric constant of fused glass beads," *Geophysics*, vol. 46, pp. 781-795, May 1981.

[12] D. Andrews and A. Bennett, "Measurements of diffusivity near the sediment-water interface with a fine-scale resistivity probe," *Geochimica et Cosmochimica ACTA*, vol. 45, pp. 2169-2175, 1981.

[13] R. H. Bennett *et al.*, "Geoacoustic and geological characterization of surfacial marine sediments by in situ probe and remote sensing techniques," in *CRC handbook of Geophysical Exploration at Sea*, 2nd Ed., R. A. Geyer, Editor, CRC Press, Boca Raton, FL, pp. 295-350, 1992.

[14] T. Yamamoto, "Velocity variabilities and other physical properties of marine sediments measured by crosswell acoustic tomography," *J. Acoust. Soc. Am.*, vol. 98, pp. 2235-2248, October 1995.